AD-786 464

A DIGITAL LEAD COMPUTING OPTICAL SIGHT MODEL

Anthony L. Leatham, et al

Air Force Academy

Prepared for:

Air Force Avionics Laboratory

September 1974

DISTRIBUTED BY:

NTIS

National Technical Information Service
U. S. DEPARTMENT OF COMMERCE
5285 Port Royal Road, Springfield Va. 22151

Unclassified

SECURITY CLASSIFICATION OF THIS PAGE (When Data Entered)

REPORT DOCUMENTATION PAGE		READ INSTRUCTIONS BEFORE COMPLETING FORM
1. REPORT NUMBER USAFA-TR-74-17	2. GOVT ACCESSION NO.	3. RECIPIENT'S CATALOG NUMBER AD 786 464
4. TITLE (and Subtitle) A DIGITAL LEAD COMPUTING optical SIGHT MODEL		5. TYPE OF REPORT & PERIOD COVERED Final Report
		6. PERFORMING ORG. REPORT NUMBER USAFA-TR-74-17
7. AUTHOR(s) Anthony L. Leatham John C. Durrett Salvatore Alfano		8. CONTRACT OR GRANT NUMBER(s)
9. PERFORMING ORGANIZATION NAME AND ADDRESS Department of Astronautics and Computer Science (DFACS) US Air Force Academy, CO 80840		10. PROGRAM ELEMENT, PROJECT, TASK AREA & WORK UNIT NUMBERS
11. CONTROLLING OFFICE NAME AND ADDRESS Dean of Faculty US Air Force Academy Colorado and Air Force Avionics Laboratory Wright-Patterson AFB, Ohio 45433		12. REPORT DATE August 1974
		13. NUMBER OF PAGES 54
14. MONITORING AGENCY NAME & ADDRESS(if different from Controlling Office)		15. SECURITY CLASS. (of this report) Unclassified
		15a. DECLASSIFICATION/DOWNGRADING SCHEDULE

16. DISTRIBUTION STATEMENT (of this Report)

Approved for public release; distribution unlimited

17. DISTRIBUTION STATEMENT (of the abstract entered in Block 20, if different from Report)

18. SUPPLEMENTARY NOTES

19. KEY WORDS (Continue on reverse side if necessary and identify by block number)

Aircraft Gunnery
Lead Computing Optical Sight
Digital Fire Control
Fire Control Algorithm

20. ABSTRACT (Continue on reverse side if necessary and identify by block number)

The equations for the lead computing optical sight are developed for implementation in an on-board digital computer. It is shown that fewer assumptions are necessary if the total nongravitational acceleration vector is available from on-board measurements. The equations are also considerably simpler if the angular rate vector of the aircraft is available from either a strapdown or inertial navigation system rather than from the lead computing gyroscope

DD FORM 1 JAN 73 1473 EDITION OF 1 NOV 65 IS OBSOLETE

Unclassified

SECURITY CLASSIFICATION OF THIS PAGE (When Data Entered)

20. in current use. Numerical comparisons are made with a digital model of the lead computing optical sight currently employed on an advanced fighter aircraft, a digital lead computing optical sight developed by Honeywell, Inc., a digital lead computing sight developed by the Air Force Avionics Laboratory, and the historical tracer sight, "HOTLINE", also developed by Honeywell, Inc. The effects of aircraft roll rate on the lead angle are correctly modeled, which results in significant improvement of the lead angle prediction during maneuvers involving roll. The equations developed are also useful in the implementation of a director type gunsight where the angular rate of the line of sight is measured directly by a tracking device.

Editorial Review by Lt. Colonel W. A. Belford, Jr.
Department of English and Fine Arts
USAF Academy, Colorado 80840

This research report is presented as a competent treatment of the subject, worthy of publication. The United States Air Force Academy vouches for the quality of the research, without necessarily endorsing the opinions and conclusions of the author.

This report has been cleared for open publication and/or public release by the appropriate Office of Information in accordance with AFR 190-17 and DODD 5230.9. There is no objection to unlimited distribution of this report to the public at large, or by DDC to the National Technical Information Service.

This research report has been reviewed and is approved for publication.

Philip J Erdle

PHILIP J. ERDLE, Colonel, USAF
Vice Dean of the Faculty

Additional copies of this document are available through the National Technical Information Service, U.S. Department of Commerce, 5285 Port Royal Road, Springfield, VA 22151.

TABLE OF CONTENTS

LIST OF TABLES

LIST OF FIGURES

LIST OF SYMBOLS

Symbol	Definition
$\bar{a}$	Unit vector along the aircraft velocity vector
$\bar{a}_N$	Total nongravitational acceleration
[A]	Coefficient matrix (3 x 3)
A_β	Variable relating drag effect to gravity drop
b	A coefficient
$\bar{b}$	Unit vector along the gunline
[B]	Coefficient matrix (3 x 3)
$\bar{c}$	Unit vector in direction of bullet velocity relative to airmass
D	Present target range
$\dot{D}$	Range rate
$\ddot{D}$	Rate of change of range rate
D_f	Future target range
$\bar{D}$	Drag
g, G	Gravity constant, 32.2 ft/sec
$\bar{g}$	Gravity vector
J_v	Variable associated with angle of attack effect on lead angle
K	Sight sensitivity parameter
$\bar{K}$	Vector relating $\bar{\lambda}$ and $\bar{b}$
$\hat{k}$	Unit vector in vertical direction (positive up)
m	Aircraft mass

Symbol	Definition
p,q,r	Gun angular rates about the aircraft x, y, z axes
$\bar{s}$	Unit vector in the direction of the target
T_f	Bullet time of flight
V, V_a	Aircraft speed
V_c	Closing speed $(-\dot{R})$
V_f	Average bullet speed
V_m	Bullet muzzle speed w.r.t. gun
$\bar{V}_T$	Target velocity
$\dot{\bar{V}}_T$	Target acceleration
$[W]$	Coefficient matrix (2 x 2)
$[W]^{-1}$	Inverse of $[W]$
$\ddot{x},\ddot{y},\ddot{z}$	Aircraft acceleration components along body axes
$\bar{z}$	Unit vector in vertical direction (positive up)
α	Aircraft angle of attack considered as a scalar
$\bar{\alpha}$	Aircraft angle of attack vector
$\bar{\alpha}_G$	Gun angle of attack vector
$\dot{\bar{\beta}}$	Sight line angular rate vector
$\dot{\bar{\beta}}'$	Normal sight line angular rate vector
$\ddot{\bar{\beta}}$	Sight line angular acceleration

Symbol	Definition
$\ddot{\bar{\beta}}'$	Normal sight line angular acceleration
δ	Radial error in mils between LCOS reticle and "HOTLINE" bullet at target range
ΔAz, ΔEl	Azimuth and elevation error in mils between LCOS reticle and "HOTLINE" bullet at target range
Δ	Determinant of [W]
$\bar{\lambda}$	Lead angle vector $(\lambda_1, \lambda_2, \lambda_3)^T$
$\dot{\bar{\lambda}}$	Lead angle rate vector
$\tilde{\lambda}$	Second and 3rd components of $\bar{\lambda}$ $(\lambda_2, \lambda_3)^T$
$\dot{\tilde{\lambda}}$	Rate of change of $\tilde{\lambda}$
$\bar{\omega}$, $\bar{\omega}(t)$	Gun angular rate vector $(p,q,r)^T$
$[\Omega]$	Coefficient matrix (2 x 3)
τ	Dummy time variable
$\bar{\theta}_G$	Gun angle vector

I. INTRODUCTION

With the installation of digital computers on fighter aircraft comes a computational capability that allows greater accuracy in the solution of fire control problems as well as greater versatility in implementing the solutions.

This report is concerned with the feasibility of implementing the solution of the lead computing optical sight (LCOS) in an on-board digital computer. For purposes of this report this sight will be called Air Force Academy LCOS (AFALCOS). It is shown that the lead angle equation required for reticle displacement on the heads-up display (HUD) can readily be solved on the digital computer. The solution of the lead angle equation is compared to the steady state solutions from models of a present day advanced fighter LCOS, the Honeywell, Inc. digital LCOS, the Avionics Laboratory digital LCOS documented in reference [2][1], and Honeywell's historical tracer sight "HOTLINE." The AFALCOS is shown to be generally more accurate that the above LCOS's and in the steady state to compare very favorably with HOTLINE.

It should be noted that comparing two generically different types of gunsights requires not only a steady state comparison for accuracy but also a dynamic comparison in which the entire pilot, target, sight display, flight control system

[1]Air-to-Air Gun Fire Control Equations for Digital Lead Computing Optical Sights, AFAL-TM-74-9-NVE-1, Apr 1974, Air Force Avionics Laboratory, Wright-Patterson AFB, Ohio.

Preceding page blank

and aerodynamic response of the aircraft are included. This complex interaction is highly coupled and the entire system needs to be tested before suitability of any one sight can be fully determined. In this report only the steady state comparison will be made.

In Section II the problem definition is presented. The assumptions are stated, and the development of the equations is made in Section III. A discussion of the problem of implementation is made in Section IV. Numerical results demonstrating the feasibility of the digital LCOS are presented in Section V as well as an accuracy comparison with the models stated above. Conclusions are stated in Section VI.

II. PROBLEM DEFINITION

Definition of LCOS

In the lead-computing gunsight, a prediction angle is continually computed and displayed on the Heads Up Display (HUD) as a reticle offset from a fixed reference on the gunsight. A typical reticle presentation on the HUD is shown in Figure 1.

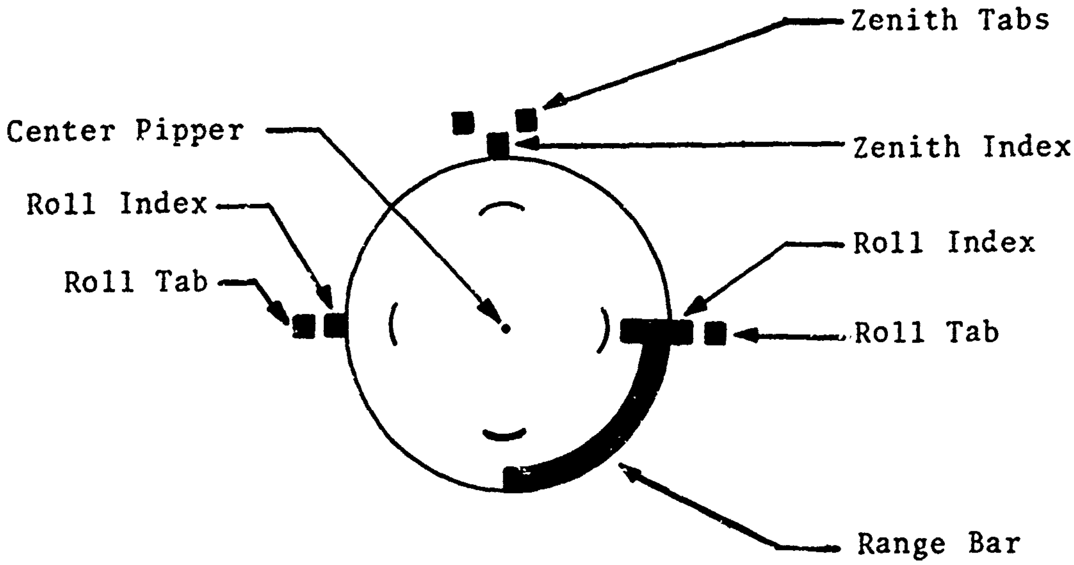

Figure 1. Typical Sight Reticle Display

The prediction angle displaces the reticle in azimuth and elevation and is the angle between the present line of sight (if the pilot has the reticle superimposed on the target) and weapon line. The prediction angle accounts

for ballistic curvature, own motion, and predicted target motion. In the implementation of this system, several drawbacks are apparent. One is the necessity to predict future target motion so that the proper lead angle may be obtained. To make a prediction, some assumptions must be made concerning future target motion which are not always valid if the target is performing evasive maneuvers. Also, the reticle, if undamped, moves abruptly in the HUD due to abrupt control inputs which are common in combat. To overcome this movement, damping must be induced in the reticle, which has the adverse effect of making the reticle lag behind real time. Thus, time is needed for the on-board computer to settle to a solution. This settling may never occur if aircraft attitude and velocity are constantly changing. LCOS, therefore, has limitations which are undesirable. However, LCOS has proven itself worthy in close-in air combat and is a usable sight.

The sight presently incorporates the use of a Lead Computing Gyroscope (LCG) which can be eliminated if the aircraft has either a strapdown or inertial navigation system on board which will provide the aircraft body rate vector. The problem, then, lies in developing a digital program capable of taking the place of the present LCOS, including the lead computing gyroscope. This approach should yield a gunsight which is more accurate than the present one at a decreased initial cost and a reduced maintenance cost.

III. DERIVATION OF LCOS EQUATIONS

In this section the lead angle equations will be developed along with the time of flight equation. Results of reference [1][1] are used extensively.

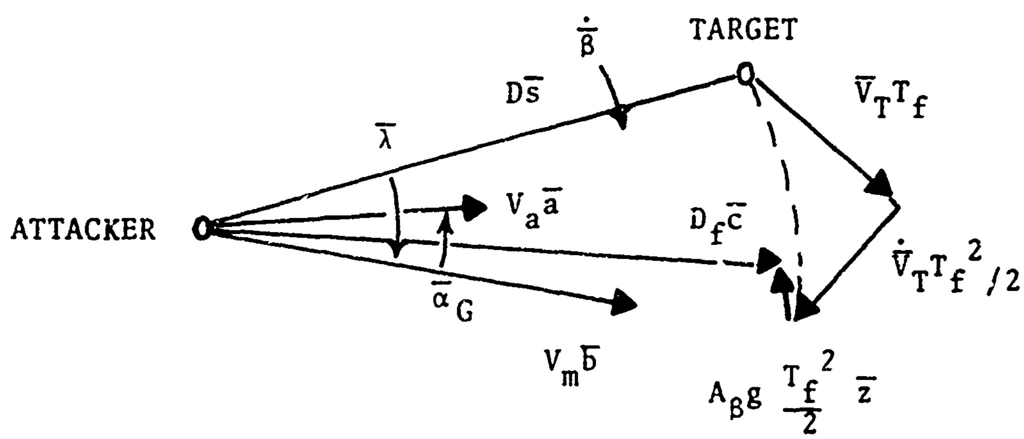

Figure 2. Lead Angle Components

From inspection of Figure 2,

$$D\bar{s} + \bar{V}_T T_f + (\dot{\bar{V}}_T + A_\beta\, g\, \bar{z})\, T_f^{\,2}/2 = D_f \bar{c}. \tag{1}$$

For the small angles involved,

$$(V_a + V_m)\, \bar{c} \cong V_a\, \bar{a} + V_m\, \bar{b} \tag{2}$$

$$\bar{c} \approx \frac{V_a}{V_a+V_m}\, \bar{a} + \frac{V_m}{V_a+V_m}\, \bar{b} \qquad \text{(Assumption).}$$

By the definitions of the four variables

$$D_f = (V_a + V_f)\, T_f. \tag{3}$$

Substitute equations (2) and (3) into equation (1) to obtain

[1] F-4E Lead Computing Optical Sight System (LCOSS) Improvement Study, Report MDC A0610 1 June 1971, Mc Donnell Aircraft Company, St. Louis, Missouri.

$$V_m T_f \left(\frac{V_a+V_f}{V_a+V_m}\right)\bar{b} = D\bar{s} + \bar{V}_T T_f + (\dot{\bar{V}}_T + A_\beta\ g\ \bar{z})T_f{}^2/2 \tag{4}$$

$$- V_a T_f \left(\frac{V_a+V_f}{V_a+V_m}\right)\bar{a}\ .$$

Lead angle $\bar{\lambda}$ considered as vector ($|\lambda|<<1$) is approximately

$$\bar{\lambda} = \bar{s} \times \bar{b} \qquad \text{(Assumption).} \tag{5}$$

Thus by crossing $\bar{s}$ into both sides of (4)

$$V_m T_f \left(\frac{V_a+V_f}{V_a+V_m}\right)\bar{\lambda} = (\bar{s} \times \bar{V}_T)\ T_f + \left[\bar{s} \times \dot{\bar{V}}_T + A_\beta\ g\ (\bar{s} \times \bar{z})\right] T_f{}^2/2$$

$$- T_f V_a \frac{V_a+V_f}{V_a+V_m} (\bar{s} \times \bar{a}). \tag{6}$$

Divided through by T_f, Equation (6) becomes

$$V_m \left(\frac{V_a+V_f}{V_a+V_m}\right)\bar{\lambda} = \bar{s} \times \left[\bar{V}_T - V_a\left(\frac{V_a+V_f}{V_a+V_m}\right)\bar{a}\right]$$

$$+ \left[\bar{s} \times \dot{\bar{V}}_T + A_\beta\ g\ (\bar{s} \times \bar{z})\right]\ T_f/2. \tag{7}$$

The first term on the right hand side (inside the brackets) is

$$\bar{V}_T - \frac{V_a\ (V_a+V_f)}{V_a+V_m}\ \bar{a} = \bar{V}_T - \frac{V_a{}^2+V_aV_m-V_aV_m+V_aV_f}{V_a + V_m}\ \bar{a}$$

$$= \bar{V}_T - V_a\bar{a} + V_a \left(\frac{V_m-V_f}{V_a+V_m}\right)\bar{a} \tag{8}$$

but;

$$\bar{V}_T - V_a\ \bar{a} = \frac{d}{dt}\ (D\bar{s}) = D\dot{\bar{s}} + \dot{D}\bar{s} \tag{9}$$

and cross both sides of (9) with $\bar{s}$ (remember $\bar{s} \times \bar{s} = 0$)

$$\bar{s} \times (\bar{V}_T - V_a\ \bar{a}) = D\ (\bar{s} \times \dot{\bar{s}}) \cong D\ [\dot{\bar{\beta}} - (\dot{\bar{\beta}} \cdot \bar{s})\bar{s}]. \tag{10}$$

The term in brackets on the r.h.s. of Eq (10) was simplified to just $\dot{\bar{\beta}}$ in previous LCOS developments, which led to an incorrect result in the effect of aircraft roll rate on the lead angle.

NOTE: $\dot{\bar{s}} = \dot{\bar{\beta}} \times \bar{s}$ (derivative of a unit vector)

cross both sides with $\bar{s}$

$\bar{s} \times \dot{\bar{s}} = \bar{s} \times (\dot{\bar{\beta}} \times \bar{s})$ and $\bar{s} \times \dot{\bar{s}} = \dot{\bar{\beta}} - (\dot{\bar{\beta}} \cdot \bar{s})\ \bar{s}$

$$\text{and} \quad \bar{s} \times \bar{a} = \bar{\lambda} + (\bar{b} \times \bar{a}) = \bar{\lambda} + \bar{\alpha}_G \tag{11}$$

where $\bar{s} \times \bar{b} \cong \bar{\lambda}$ (Assumption)

$\bar{b} \times \bar{a} \cong \bar{\alpha}_G$ (Assumption).

Substitute equations (8), (10), and (11) into (7) to obtain

$$V_m \left(\frac{V_a + V_f}{V_a + V_m}\right) \bar{\lambda} = \bar{s} \times \left[\bar{V}_T - V_a\ \bar{a}\right] + V_a \left(\frac{V_m - V_f}{V_a + V_m}\right) (\bar{s} \times \bar{a}) \tag{12}$$

$$+ (\bar{s} \times \dot{\bar{V}}_T)\ T_f/2 + A_\beta\ g\ (\bar{s} \times \bar{z})\ T_f/2$$

$$= D\ [\dot{\bar{\beta}} - (\dot{\bar{\beta}} \cdot \bar{s})\bar{s}] + \frac{V_a(V_m - V_f)}{V_a + V_m} (\bar{\lambda} + \bar{\alpha}_G)$$

$$+ (\bar{s} \times \dot{\bar{V}}_T)\ T_f/2 + A_\beta\ g\ (\bar{s} \times \bar{z})\ T_f/2. \tag{13}$$

Collect terms in $\bar{\lambda}$:

$$V_f \bar{\lambda} = D\dot{\bar{\beta}}' + J_v V_a \bar{\alpha}_G + A_\beta\ g\ (\bar{s} \times \bar{z})\ T_f/2 + (\bar{s} \times \dot{\bar{V}}_T)\ T_f/2 \tag{14}$$

where

$$Jv = \frac{V_m - V_f}{V_a + V_m} \text{ and } \dot{\bar{\beta}}' = \dot{\bar{\beta}} - (\dot{\bar{\beta}} \cdot \bar{s})\ \bar{s}. \tag{15}$$

Target acceleration is the only component of lead which is not expressed directly in terms of quantities measurable on board the aircraft. The next objective is to relate target acceleration to those parameters which can be either effectively measured or estimated.

From equation (9),

$$\dot{\bar{V}}_T = \dot{V}_a\,\bar{a} + \frac{d}{dt}(D\dot{\bar{s}}) = \dot{V}_a\,\bar{a} + D\ddot{\bar{s}} + \dot{D}\dot{\bar{s}}. \tag{16}$$

At this point, previous derivations of LCOS have assumed constant target and attacker speeds; however, this assumption is not necessary unless only the normal acceleration is measured. Proceeding without this assumption, we can write

$$\dot{\bar{V}}_T = \frac{d}{dt}(V_a\bar{a}) + \frac{d}{dt}(D\,\dot{\bar{\beta}} \times \bar{s}) + \frac{d}{dt}(\dot{D}\bar{s}). \tag{17}$$

We now write Newton's second law for the attacker,

$$\bar{T} + \bar{D} + \bar{L} + \bar{W} = m\,\frac{d}{dt}(V_a\bar{a}). \tag{18}$$

Rearranging (18) we have

$$\frac{d}{dt}(V_a\bar{a}) = (\bar{T} + \bar{D} + \bar{L})/m + \bar{g}. \tag{19}$$

The right hand side of (19) is arranged in the manner shown because an on-board accelerometer triad will measure only nongravitational accelerations. Let $\bar{a}_N$ denote the nongravitational accelerations,

$$\bar{a}_N = (\bar{T} + \bar{D} + \bar{L})/m. \tag{20}$$

Equation (19) becomes

$$\frac{d}{dt}(V_a\bar{a}) = \bar{a}_N + \bar{g}. \tag{21}$$

Substituting Equation (21) into Equation (17) and taking the vector cross product of both sides of equation (17) results in

$$\bar{s} \times \dot{\bar{V}}_T = \bar{s} \times (\bar{a}_N + \bar{g}) + 2\dot{D}\,\bar{s} \times (\dot{\bar{\beta}} \times \bar{s}) + D\,\bar{s} \tag{22}$$

$$\times [\dot{\bar{\beta}} \times (\dot{\bar{\beta}} \times \bar{s})] + D\,\bar{s} \times (\ddot{\bar{\beta}} \times \bar{s}) + \ddot{D}\,\bar{s} \times \bar{s}.$$

Noting that

$$\bar{s} \times \bar{s} = 0$$

$$\bar{s} \times \dot{\bar{s}} = \dot{\bar{\beta}} - (\dot{\bar{\beta}} \cdot \bar{s})\,\bar{s} = \dot{\bar{\beta}}'$$

$$\bar{s} \times \ddot{\bar{s}} = \ddot{\bar{\beta}}' = \ddot{\bar{\beta}} - (\ddot{\bar{\beta}} \cdot \bar{s})\,\bar{s}.$$

Applying the rule for a vector triple product, Equation (22) can be rewritten

$$\bar{s} \times \dot{\bar{V}}_T = \bar{s} \times (\bar{a}_N + \bar{g}) + 2\dot{D}\,[\dot{\bar{\beta}} - (\dot{\bar{\beta}} \cdot \bar{s})\bar{s}] + D(\dot{\bar{\beta}} \cdot \bar{s})\bar{s} \times \dot{\bar{\beta}} \tag{23}$$

$$+ D[\ddot{\bar{\beta}} - (\ddot{\bar{\beta}} \cdot \bar{s})\,\bar{s}].$$

Substituting the r.h.s. of equation (23) for the term $\bar{s} \times \dot{\bar{V}}_T$ in the r.h.s. of equation (14), we have an equation which no longer contains any terms referring to the target except $\bar{s}$, the line of sight unit vector,

$$\bar{\lambda} = \frac{D+T_f\dot{D}}{V_f}\,\dot{\bar{\beta}}' + \frac{T_f}{2V_f}\,D(\dot{\bar{\beta}} \cdot \bar{s})\,\bar{s} \times \dot{\bar{\beta}} + J_V\frac{V_a}{V_f}\,\bar{\alpha}_G + \frac{T_f}{2V_f}\,\bar{s} \times \bar{a}_N$$

$$-(1-A_\beta)\frac{T_f}{2V_f}\,g\,\bar{s} \times \bar{z} + D\,\frac{T_f}{2}\,\ddot{\bar{\beta}}' \tag{24}$$

where

$$\ddot{\bar{\beta}}' = \ddot{\bar{\beta}} - (\ddot{\bar{\beta}} \cdot \bar{s})\,\bar{s}.$$

Since $\bar{s}$ is not measurable without an accurate tracking device, $\bar{s}$ must be determined in terms of other measurable quantities. From equation (5)

$$\bar{\lambda} = \bar{s} \times \bar{b}$$

and since $|\bar{\lambda}| << 1$ let us define a vector $\bar{k}$ such that

$$\bar{k} = \bar{b} \times \bar{\lambda} \tag{25}$$

where $\bar{b}$ is the gunline unit vector. From Figure 3 it is clear that

$|\bar{k}| \approx \lambda$ and

$$\bar{s} \approx \bar{b} + \bar{k} = \bar{b} + (\bar{b} \times \bar{\lambda}). \tag{26}$$

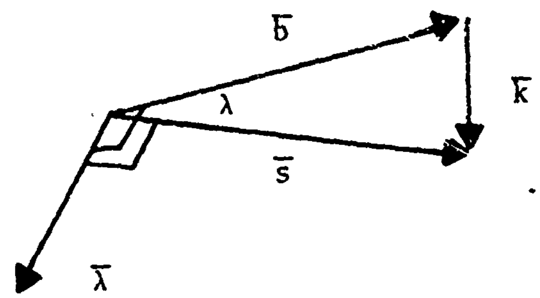

Figure 3. Relationship of $\bar{\lambda}$, $\bar{s}$, $\bar{b}$, and $\bar{k}$

In the r.h.s. of equation (24) we can express $\bar{s} \times \bar{a}_N$ in terms of $\bar{a}_N$, $\bar{b}$, and $\bar{\lambda}$, all of which can be measured or computed on board the attacker aircraft,

$$\bar{s} \times \bar{a}_N = [\bar{b} + (\bar{b} \times \bar{\lambda})] \times \bar{a}_N \tag{27}$$

$$= \bar{b} \times \bar{a}_N - (\bar{a}_N \cdot \bar{\lambda})\bar{b} + (\bar{a}_N \cdot \bar{b})\bar{\lambda}.$$

Next we consider $\dot{\bar{\beta}}$. Referring to Figure 4 we can write

$$\dot{\bar{\beta}} \cong \bar{\omega} - \dot{\bar{\lambda}} \qquad \text{(Assumption).} \tag{28}$$

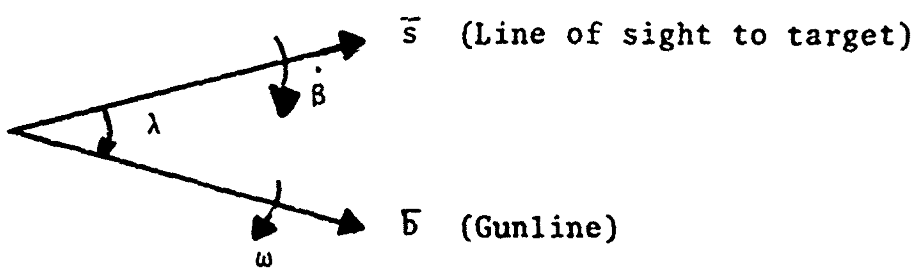

Figure 4. Geometrical Relationship Between $\dot{\bar{\beta}}$, $\bar{\omega}$, and $\bar{\lambda}$

We now need to simplify the terms in equation (24) containing $\dot{\bar{\beta}}$ which are

$$(D + T_f D) \; [\dot{\bar{\beta}} - (\dot{\bar{\beta}} \cdot \bar{s})\bar{s}] + \frac{T_f}{2} D \; (\dot{\bar{\beta}} \cdot \bar{s})\bar{s} \times \dot{\bar{\beta}}. \qquad (29)$$

The term $[\dot{\bar{\beta}} - (\dot{\bar{\beta}} \cdot \bar{s})\bar{s}]$ can be written in matrix form as

$$\dot{\bar{\beta}}' = [\dot{\bar{\beta}} - (\dot{\bar{\beta}} \cdot \bar{s})\bar{s}]$$

$$= \begin{bmatrix} (1-s_1^2) & -s_1 s_2 & -s_1 s_3 \\ -s_1 s_2 & (1-s_2^2) & -s_2 s_3 \\ -s_1 s_3 & -s_2 s_3 & (1-s_3^2) \end{bmatrix} \dot{\bar{\beta}}$$

$$= [A] \; \dot{\bar{\beta}}. \qquad (30)$$

The term $\bar{s} \times \dot{\bar{\beta}}$ can be written in matrix form as

$$\bar{s} \times \dot{\bar{\beta}} = \begin{bmatrix} 0 & -s_3 & s_2 \\ s_3 & 0 & -s_1 \\ -s_2 & s_1 & 0 \end{bmatrix} \dot{\bar{\beta}}$$

$$= [B] \; \dot{\bar{\beta}}. \qquad (31)$$

Finally, we assume that

$$\dot{\bar{\beta}} \cdot \bar{s} = p \qquad \text{(Assumption)} \qquad (32)$$

where p is the roll rate of the aircraft.

This assumption is very reasonable since $\dot{\bar{\beta}}$ is the angular rate vector of the line of sight and $\dot{\bar{\beta}} \cdot \bar{s}$ is simply the component of angular rate along the line of sight.

The line of sight vector $\bar{s}$ is nearly aligned with the roll axis of the aircraft.

The expression (29) can now be written

$$(D + T_f\dot{D})[A]\dot{\bar{\beta}} + \frac{T_f}{2} D\ p\ [B]\ \dot{\bar{\beta}}$$

$$= (D + T_f\dot{D})\{[A] + \frac{T_f Dp}{2(D+T_f\dot{D})} [B]\}\ \dot{\bar{\beta}} \qquad (33)$$

$$= (D+T_f\dot{D})\ \{A + bB\}\ \dot{\bar{\beta}}.$$

Substituting equation (33) and equation (28) into the lead angle equation Eq (24) results in

$$V_f\bar{\lambda} = (D+T_f\dot{D})\ \{A + bB\}\ (\bar{\omega}-\dot{\bar{\lambda}}) + J_vV_a\ \bar{\alpha}_G + \frac{T_f}{2}\ \bar{s} \times \bar{a}_N \qquad (34)$$

$$+ (1-A_\beta)\frac{T_f}{2}\ g\ \bar{s} \times \bar{z} + D\ \frac{T_f}{2}\ [A]\ \ddot{\bar{\beta}}\ .$$

The last two terms are neglected in current LCOS mechanization and will be neglected here since the terms $(1-A_\beta)$ and $|\ddot{\bar{\beta}}|$ are generally very small. We desire a differential equation for the lead angle; therefore, we solve for $\dot{\bar{\lambda}}$. Rearranging Eq (34) and neglecting the last two terms

$$\{A+bB\}\dot{\bar{\lambda}} = \{A+bB\}\bar{\omega} - \frac{V_f}{(D+T_f\dot{D})}\ \bar{\lambda} + \frac{J_vV_a}{(D+T_f\dot{D})}\ \bar{\alpha}_G \qquad (35)$$

$$+ \frac{T_f}{2(D+T_f\dot{D})}\ \bar{s} \times \bar{a}_N\ .$$

To solve for $\dot{\bar{\lambda}}$ it is necessary to invert the matrix {A+bB}; however, this matrix is singular if the line of sight vector corresponds with the aircraft body axis. The matrix {A+bB} multiplying $\dot{\bar{\lambda}}$ in Eq (35) can be written

$$\{A+bB\} = \begin{bmatrix} (1-s_1^2) & -(s_1 s_2 + bs_3) & (-s_1 s_3 + bs_2) \\ (-s_1 s_2 + bs_3) & (1-s_2^2) & -(s_2 s_3 + bs_1) \\ -(s_1 s_3 + bs_2) & (-s_2 s_3 + bs_1) & (1-s_3^2) \end{bmatrix} . \tag{36}$$

Note that if $s_1=1$, $s_2= s_3= 0$, then the first row of {A+bB} is zero, and the matrix is singular. This problem can be circumvented by deleting the first component equation for $\dot{\lambda}_1$ since λ_1 is not required for displaying the lead angle. However, before deleting the first row and column of {A+bB} it is necessary to first multiply the matrices {A+bB} $\bar{\omega}$ on the r.h.s. of Eq (35). This multiplication introduced the effect of roll, p, into the equations for $\dot{\lambda}_2$ and $\dot{\lambda}_3$. The resulting equation is

$$\begin{bmatrix} (1 \; s_1^2) & -(s_2 s_3 + bs_1) \\ (-s_2 s_3 + bs_1) & (1-s_3^2) \end{bmatrix} \begin{pmatrix} \dot{\lambda}_2 \\ \dot{\lambda}_3 \end{pmatrix} = [W] \begin{pmatrix} \dot{\lambda}_2 \\ \dot{\lambda}_3 \end{pmatrix}$$

$$= \begin{bmatrix} (-s_1 s_2 + bs_3)\omega_1 + (1-s_2^2)\omega_2 - (s_2 s_3 + bs_1)\omega_3 \\ (-s_1 s_3 + bs_2)\omega_1 + (-s_2 s_3 + bs_1)\omega_2 + (1-s_3^2)\omega_3 \end{bmatrix} + \frac{J_v V_a}{(D+T_f \dot{D})} \overline{\alpha_G}$$

$$+ \frac{T_f}{2(D+T_f \dot{D})} \bar{s} \times \bar{a}_N - \frac{V_f}{D+T_f \dot{D}} \bar{\lambda} . \tag{37}$$

The inverse of the matrix [W] is

$$[W]^{-1} = \frac{1}{\Delta}\begin{bmatrix}(1-s_3^2) & (s_2 s_3+bs_1)\\ (s_2 s_3-bs_1) & (1-s_2^2)\end{bmatrix} \tag{38}$$

where

$$\Delta = 1-s_2^2 - s_3^2 + b^2 s_1^2. \tag{39}$$

The differential equations for $\dot{\lambda}_2$ and $\dot{\lambda}_3$ can now be written

$$\dot{\tilde{\lambda}} = [W]^{-1}\left\{[\Omega]\bar{\omega} - \frac{V_f}{D+\dot{D}T_f}\tilde{\lambda} + \frac{J_v V_a}{D+\dot{D}T_f}\bar{\alpha}_G + \frac{T_f}{2(D+T_f\dot{D})}\bar{s}\times\bar{a}_N\right\} \tag{40}$$

where

$$\tilde{\lambda} = \begin{pmatrix}\lambda_2\\ \lambda_3\end{pmatrix} \tag{41}$$

and

$$[\Omega] = \begin{bmatrix}(-s_1 s_2+bs_3) & (1-s_2^2) & -(s_2 s_3+bs_1)\\ -(s_1 s_3+bs_2) & (-s_2 s_3+bs_1) & (1-s_3^2)\end{bmatrix}. \tag{42}$$

Finally, substituting for $\bar{s}$ from Eq (27) into Eq (40) we obtain the lead angle equation

$$\dot{\tilde{\lambda}} = [W]^{-1}\left\{[\Omega]\bar{\omega} - \frac{V_f}{(D+\dot{D}T_f)}\tilde{\lambda} + \frac{J_v V_a}{D+\dot{D}T_f}\bar{\alpha}_G + \frac{T_f}{2(D+T_f\dot{D})}[\bar{b}\times\bar{a}_N - (\bar{a}_N\cdot\bar{\lambda})\bar{b}\right.$$

$$\left. + \bar{a}_N\cdot\bar{b}\tilde{\lambda}]\right\} \tag{43}$$

where $\lambda_1 = 0$ in $\bar{a}_N\cdot\bar{\lambda}$.

This is the equation which will be mechanized with some further simplifications, depending upon sensor information and geometric orientation of the gun in the aircraft. These items will be discussed further in section IV.

Derivation of T_f and V_f

T_f and V_f are respectively the bullet time of flight and average bullet velocity relative to the attacker.

An empirical model which is sufficiently accurate for bullet time of flight is

$$T_f = R_F/(V_p - K_B R_F V_p^{\frac{1}{2}} \rho/\rho_o) \quad (44)$$

where R_F is the final range determined by

$$R_F = R + (V_a + \dot{R})T_f \, . \quad (45)$$

V_p is the initial projectile speed in the airmass.

K_B is an empirically derived ballistic coefficient.

ρ/ρ_o is the density ratio.

By substituting equation (31) into equation (30) we obtain

$$T_F = \frac{\left[R + (V_a + \dot{R})T_f\right]}{\left\{V_p - K_B \left[R + (V_a + \dot{R})T_f\right] V_p^{\frac{1}{2}} \rho/\rho_o\right\}} \, . \quad (46)$$

Let

$$V_{LS} \equiv RK_B V_p^{\frac{1}{2}} \rho/\rho_o \, . \quad (47)$$

Equation (46) is a quadratic in T_F when both sides are multiplied by the denominator of the r.h.s.,

$$\left[K_B (V_a - V_c)V_p^{\frac{1}{2}} \rho/\rho_o\right] T_f^2 + \left[V_{LS} - (V_p - V_a) + \dot{R}\right]T_f + R = 0 \quad (48)$$

Let

$$V_{os} = V_m - R - V_{LS} \quad (49)$$

$$V_p = V_a + V_m \quad (50)$$

and divide both sides of equation (48) by T_f^2

$$R\left(\frac{1}{T_f}\right)^2 - V_{os}\left(\frac{1}{T_f}\right) + \left[K_B(V_a + \dot{R})V_p^{\frac{1}{2}}\, {}^{\rho}/\rho_o\right] = 0 \tag{51}$$

$$\frac{1}{T_f} = \frac{V_{os} + \sqrt{V_{os}^2 - 4V_{LS}(V_a + \dot{R})}}{2R} . \tag{52}$$

Letting

$$V_{cm} = \sqrt{V_{os}^2 - 4V_{LS}(V_a - V_c)} \tag{53}$$

then

$$T_f = \frac{2R}{V_{os} + V_{cm}} . \tag{54}$$

Equation (54) is used to calculate time of flight T_f for the lead angle equation, equation (43). To obtain V_f, the average bullet speed with respect to the attacker,

$$V_f \approx \frac{D_f}{T_f} - V_a \tag{55}$$

$$= \left[D + (V_a + \dot{R})T_f\right] /T_f - V_a$$

$$V_f = D/T_f + \dot{R} . \tag{56}$$

Equation (56) is used to compute V_f for the lead angle equation, equation (43).

Note in equations (53) and (54) that V_{cm}; hence, T_f may be undefined if the argument of the square root is negative. This situation can occur for certain engagement conditions and must be checked for solution validity.

IV. IMPLEMENTATION OF LCOS EQUATIONS

In practice, the $\bar{z}$ vector may not be available. The term containing $\bar{z}$ is very small in any case (ref 1); hence, this term is often neglected. The $\ddot{\bar{\beta}}$ vector can be obtained by differentiating $\dot{\bar{\beta}}$ in equation (28); however, because differentiation is a noisy process and this term is a second order effect significant only during transient maneuvers when tracking is extremely difficult, this term is generally neglected. For the remainder of this report, the terms containing $\bar{z}$ and $\ddot{\bar{\beta}}$ will be dropped as in earlier LCOS mechanizations. A later investigation is planned to determine the consequences of neglecting these terms.

Equation (43) can be integrated on an on-board digital computer to obtain the lead angle $\tilde{\lambda}(t)$. The speed of integration can be modified to obtain better sight stability by time scaling equation (43). Let the new time variable τ be defined such that

$$t = K\tau, \; dt = Kd\tau \; . \tag{57}$$

Substituting Eq (57) into Eq (43) and rearranging, we obtain

$$\frac{d\tilde{\lambda}}{d\tau} = K[W]^{-1}\Big\{[\Omega]\bar{\omega} - \frac{V_f\tilde{\lambda}}{(D+T_f\dot{D})} + \frac{T_f}{2(D+T_f\dot{D})}[\bar{b} \times \bar{a}_N - (\bar{a}_N \cdot \bar{\lambda})\bar{b} + (\bar{a}_N \cdot \bar{b})\tilde{\lambda}] + \frac{J_v V_a}{(D+\dot{D}T_f)}\bar{\alpha}_G\Big\} . \tag{58}$$

Equation (58) is a first order differential equation linear in $\tilde{\lambda}$. The terms not containing $\tilde{\lambda}$ can be regarded as forcing terms, since they are dependent upon the attacker's maneuvers.

If steady state conditions exist, $\frac{d\tilde{\lambda}}{d\tau}$ will approach zero, and a steady state value of $\tilde{\lambda}$ can be obtained by integrating equation (44) until $\frac{d\tilde{\lambda}}{d\tau} \approx 0$, or, alternatively, $\frac{d\tilde{\lambda}}{d\tau}$ can be set to zero, and $\tilde{\lambda}$ for the steady state situation can be obtained from the resulting algebraic equation. If steady state conditions do not exist, however, $\tilde{\lambda}(t)$ obtained by integrating equation (58) will lag the actual lead angle because of the time constant associated with $\tilde{\lambda}$.

This time constant can be modified merely by changing the time scaling factor K defined in equation (57). Alternatively, K can be considered as a gain in a control system with output $\tilde{\lambda}(t)$. Increasing K decreased the time constant of $\tilde{\lambda}$ in equation (58); however, the greater K is, the greater will be the reticle sensitivity to changes in attacker aircraft acceleration, angle of attack, and rate of turn. Thus, a trade-off on the value of K is required between the pilot's ability to track a target with the reticle and the response of the reticle to changes in aircraft dynamics commanded by the pilot. The value K = .80 corresponds to the sight damping factor σ = .25 (ref 1) found in most present day LCOS.

Transient Response Versus K

The transient response of equation (58) to a step input is illustrated in Figure 5 for various values of K. Initially, $\tilde{\lambda}(t_o) = 0$, and the step input of $\bar{\omega}(t) = 0$, $\bar{a}_N(t) = -32.2\hat{k}$, $\bar{\alpha}(t) = 0$, $t>0$ corresponds to straight and level flight. Figure 5 clearly shows the lag existing in the LCOS in any nonsteady situation. The obvious result is to choose the gain K as high as possible consistent with the pilot's ability to track his target with the more responsive reticle.

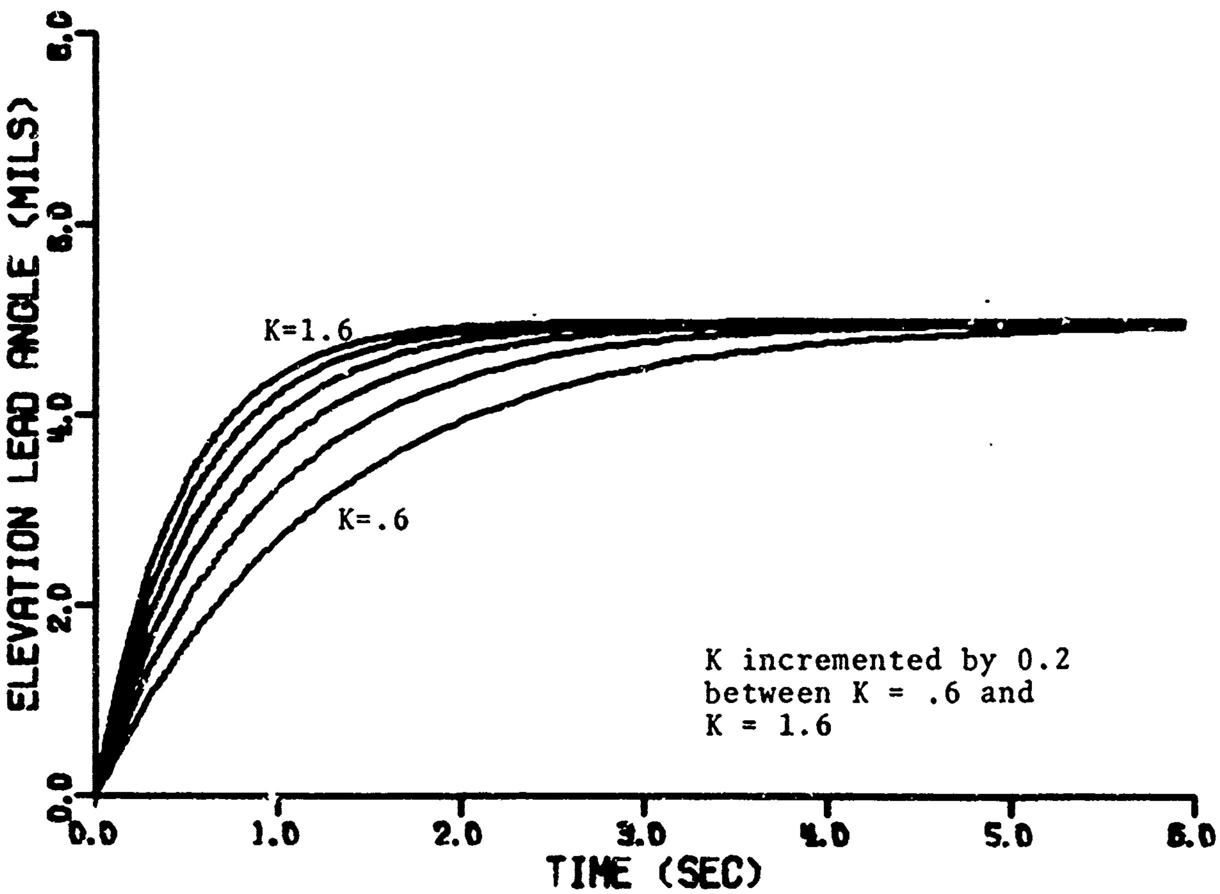

Figure 5. Transient Response of Lead Angle for Various Values of K.

Sensitivity of $\tilde{\lambda}(t)$ to Accelerations in x and y

The present LCOS measures only acceleration normal to the aircraft body x-y plane. In this report no assumption was made to measure acceleration only in the body z direction; hence, it is of interest to determine the sensitivity of the lead angle $\tilde{\lambda}(t)$ to accelerations in the body x and y directions. $\tilde{\lambda}(t)$ for various accelerations, including the body x and y accelerations, is compared in Table 1 to the lead angle generated by assuming only normal acceleration. The results show that $\tilde{\lambda}(t)$ is quite insensitive to $\ddot{x}$ while it is considerably more sensitive to $\ddot{y}$. In judging the importance of the sensitivity of $\tilde{\lambda}(t)$ to $\ddot{y}$, one must keep in mind that for coordinated flight $\ddot{y} = 0$, and for tracking situations it is most likely that the pilot will be coordinated. Therefore, LCOS can employ only normal acceleration $\ddot{z}$ with little degradation in sight accuracy provided the pilot makes coordinated turns during tracking.

Table 1. Sensitivity Of Lead Angle $\tilde{\lambda}(t)$ To Body x and y Acceleration

Range = 2000' v = 800 fps h = 10000'
Level Flight

Acceleration		Effect (Mils)	
$\ddot{x}$ (ft/sec^2)	$\ddot{y}$ (ft/sec^2)	El	Az
16.1	0.	0.	.02
32.2	0.	0.	.03
0.	8.05	1.2	0.
0.	16.1	2.5	0.

Further Simplification of Lead Angle Equations

As stated earlier, the sensor information available and the geometry of the gun placement have an effect on the complexity of the terms in Eq (58). The sensors under discussion are angle-of-attack meter and body mounted accelerometers.

Angle of Attack

Generally the angle of attack of the aircraft is measured in the body x-z plane; hence, for small angles it can be considered as a rotation about the body y axis. The angle of attack of the aircraft can then be expressed as

$$\bar{\alpha} = \begin{pmatrix} 0 \\ \alpha \\ 0 \end{pmatrix} . \qquad \text{(assuming no side slip)} \tag{59}$$

The angle of attack of the gun $\bar{\alpha}_G$ is the angle required in Eq (58), and the relationship between $\bar{\alpha}$ and $\bar{\alpha}_G$ is

$$\bar{\alpha}_G = \bar{\alpha} - \bar{\theta}_G \tag{60}$$

where $\bar{\theta}_G$ is the angle considered as a vector that the gun makes with the x axis of the aircraft. Figure 6 shows the geometrical relationship between $\bar{\alpha}_G$, $\bar{\alpha}$, and $\bar{\theta}_G$. If the gun is mounted in the body x-z plane, then

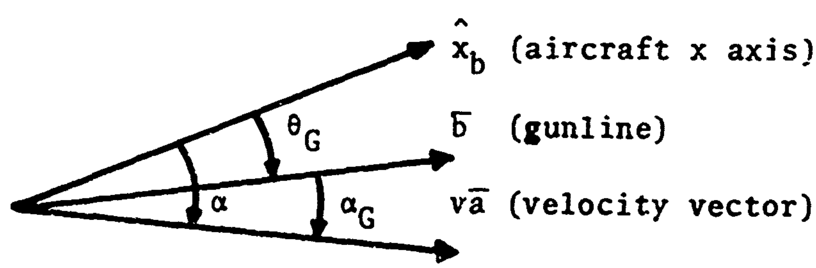

Figure 6. Geometrical relationship between $\bar{\alpha}_G$, $\bar{\alpha}$, and θ_G

$\bar{\alpha}_G$ is

$$\bar{\alpha}_G = \begin{Bmatrix} \alpha & \begin{matrix} o \\ - \\ o \end{matrix} & \theta_G \end{Bmatrix} . \tag{61}$$

Accelerometers

If only one accelerometer is employed in LCOS to measure body acceleration in the z axis, then $\bar{a}_N$ in Eq (58) is

$$\bar{a}_N = \begin{Bmatrix} \ddot{x} \\ \ddot{y} \\ \ddot{z} \end{Bmatrix} = \begin{Bmatrix} o \\ o \\ \ddot{z} \end{Bmatrix} \tag{62}$$

and the terms containing $\bar{a}_N$ simplify to

$$\bar{b} \times \bar{a}_N = -\begin{Bmatrix} b_2 \ddot{z} \\ b_1 \ddot{z} \\ o \end{Bmatrix} \tag{63}$$

$$\bar{a}_N \cdot \bar{b} = \ddot{z} b_3 \tag{64}$$

$$\bar{a}_N \cdot \bar{\lambda} = \ddot{z} \lambda_3 . \tag{65}$$

Gun Location

If the gun is located in the body x-z plane, then the gun vector $\bar{b}$ becomes

$$\bar{b} = \begin{Bmatrix} b_1 \\ o \\ b_3 \end{Bmatrix} . \tag{66}$$

V. NUMERICAL COMPARISON WITH OTHER GUNSIGHTS

A brief description of four other gunsights with which a comparison of AFALCOS will be made follows. A Fortran language listing of AFALCOS is found in Appendix A.

"HOTLINE" Historical Tracer

This gunsight is a historical tracer type sight in which the relative trajectory of the bullets with respect to the attacking aircraft is computed and displayed on a heads up display (HUD). If range is known from radar, a small reticle appears on the HUD at the point where a bullet at target range would be if it had been fired one time of flight ago - thus the name "historical tracer." Very few assumptions are made in the calculations to obtain the relative bullet stream position; therefore, this sight is considered an accurate standard for comparison purposes. The authors are grateful to Honeywell Inc. for making this sight digital program available to the Air Force. The equations and program are considered proprietary by Honeywell Inc.; hence, they are not included in this report.

Advanced Fighter LCOS

A digital model representative of the lead computing sight for a current advanced fighter aircraft was programmed by members of the Astronautics and Computer Science Department of the US Air Force Academy. This digital model includes a digital representation of the lead computing gyroscope

employed in this lead computing sight. The digital gyroscope model was programmed by the Air Force Avionics Laboratory, WPAFB, Ohio. A listing of the Fortran language digital program is found in Appendix B.

Honeywell Digital LCOS

The equations and digital program for the above advanced fighter LCOS were given to Honeywell Inc. for development of a digital LCOS to be used in the Air Force Avionics Laboratory's Comparative Gunsight Test Program in which a flight test comparison between a historical tracer type sight (HOTLINE) and an LCOS sight was to be made. Honeywell simplified the equations and digital code to develop a compact code which could be programmed on an aircraft digital computer. It should be noted that during the course of this simplification and program checkout, Honeywell's engineers discovered the roll coupling discrepancy between the advanced fighter LCOS and their own HOTLINE and brought the matter to the attention of the Air Force. A Fortran language program listing is found in Appendix C.

Air Force Avionics Laboratory LCOS

This digital LCOS was developed by the Air Force Avionics Laboratory to support the laboratory's Digital Avionics Information System (DAIS) project. This development is similar to the other digital LCOS derivations except that the small angle assumptions made in the other LCOS derivations have been avoided.

Because this LCOS uses a different time of flight equation than the other LCOS's, to obtain a better basis for comparison the bullet time of flight calculation was removed and the time of flight computed in the other LCOS's was used. It should be noted that when the original time of flight calculation is used, worse agreement is obtained between this LCOS and HOTLINE. A Fortran language listing is found in Appendix D. The development of the equations for this LCOS is found in reference [2].

Comparison

Five cases at 2000 feet of range and five cases at 3000 feet of range were used as a basis of comparison. In each case the altitude was 10000 feet, aircraft angle of attack α was zero, gun angle θ_G was zero, muzzle velocity was 3300 ft/sec, and sight damping factor σ for the Honeywell, advanced fighter, and AFAL LCOS's was 0.25. Aircraft load factor in each case was 4. The sights were allowed to settle for 12 seconds so that a steady state comparison could be made. Table 2 shows the results of the comparison at 2000' range, whereas Table 3 contains the comparisons at 3000' range. Table 4 contains the results of the comparison between HOTLINE and the AFAL LCOS at both 2000' and 3000' of range. The time of flight calculation used in the AFAL LCOS is identical to that used in the other LCOS's.

TABLE 2. Gunsight Comparison (Mils) Range = 2000'

CASES	HONEYWELL LCOS			ADV FTR LCOS			AFALCOS			HOTLINE	
	ΔAz	ΔEl	δ	ΔAz	ΔEl	δ	ΔAz	ΔEl	δ	Az	El
(1) 4-G level turn v = 600 fps	- .9	- .7	1.3	- .1	-3.5	3.5	.9	- .7	1.3	-40.1	-172.9
(2) 4-G level turn v = 800 fps	- .1	- .6	.6	.1	-3.0	3.0	.8	.6	1.0	-31.4	-138.4
(3) 4-G pullup v = 600 fps	0.	-1.1	1.1	0.	-3.6	3.6	0.	-1.1	1.1	0.	-141.6
(4) 4-G 45° Bank pullup v = 600 fps	-1.3	- .7	1.5	-1.1	-3.5	3.7	.6	- .9	1.1	-29.9	-152.3
Average Error for cases (1)-(4)			1.1			3.4			1.1		
(5) 4-G 45° Bank pullup with p = .2 rad/sec v = 600 fps	17.5	.8	17.7	21.5	-1.1	21.5	1.8	1.3	2.2	-16.8	-154.0

TABLE 3. Gunsight Comparison (Mils) Range = 3000'

CASES	HONEYWELL LCOS			ADV FTR LCOS			AFALCOS			HOTLINE	
	ΔAz	ΔEl	δ	ΔAz	ΔEl	δ	ΔAz	ΔEl	δ	Az	El
(1) 4-G level turn v = 600 fps	-7.4	-4.1	7.4	-1.2	-12.2	12.3	3.9	-4.3	5.8	-72.0	-306.5
(2) 4-G level turn v = 800 fps	-2.8	-4.0	4.9	1.5	- 9.1	9.2	3.1	-4.2	5.1	-58.1	-255.4
(3) 4-G pullup v = 600 fps	0.	-4.8	4.8	0.	- 9.4	9.4	0.	-4.8	4.8	0.	-251.5
(4) 4-G 45° Bank pullup v = 600 fps	-6.9	-3.8	7.9	-2.9	- 9.6	10.0	2.1	4.5	5.0	-54.3	-270.2
Average Error for cases (1)-(4)			6.2			10.2			5.2		
(5) 4-G 45° Bank pullup with p = .2 rad/sec v = 600 fps	54.6	12.3	56.0	65.6	12.7	66.8	9.5	5.7	11.1	-13.1	-273.7

TABLE 4. Air Force Avionics Laboratory LCOS Comparison (mils)

CASES	Range = 2000'					Range = 3000'				
	AFAL LCOS			HOTLINE		AFAL LCOS			HOTLINE	
	ΔAz	ΔEl	δ	Az	El	ΔAz	ΔEl	δ	Az	El
(1) 4-G level turn v = 600 fps	- .3	-1.4	1.4	-40.1	-172.9	- .8	-12.0	12.0	-72.0	-306.5
(2) 4-G level turn v = 800 fps	.5	- .8	.9	-31.4	-138.4	.6	- 8.1	8.1	-58.1	-255.4
(3) 4-G pullup v = 600 fps	0.	-1.3	1.3	0.	-141.6	0.	- 7.9	7.9	0.	-251.5
(4) 4-G 45° Bank pullup v = 600 fps	- .3	-1.2	1.2	-29.9	-152.3	-2.0	- 8.6	8.8	-54.3	-270.2
Average Error for cases (1)-(4)		1.2						9.2		
(5) 4-G 45° Bank pullup with p = .2 rad/sec v = 600 fps	12.0	- .5	12.0	-16.8	-154.0	38.4	1.0	38.4	-13.1	-273.7

ΔAz and ΔEl are the differences in mils between the HOTLINE sight bullet at target range as seen in a heads up display and the LCOS reticle position in the HUD. δ is the radial error which is the square root of the sum of the squares of ΔAz and ΔEl. The Azimuth and elevation of the bullet at target range from the HOTLINE sight are listed in the columns under HOTLINE. The geometry is shown in Figure 7.

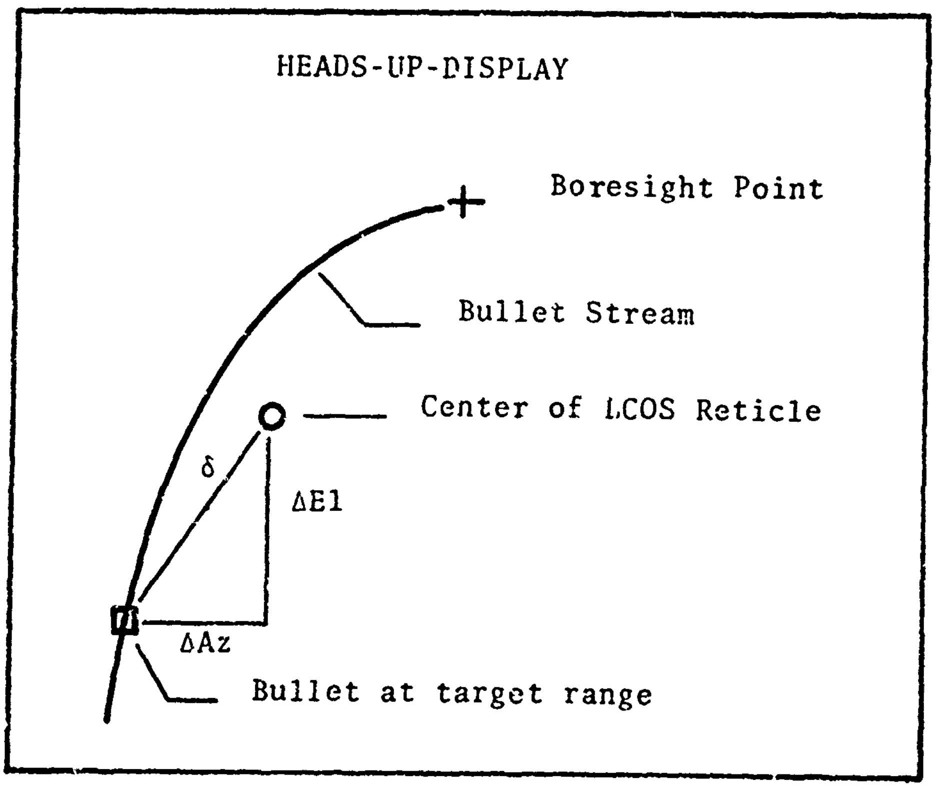

Figure 7. Errors ΔAz, ΔEl, and δ for Table 2, 3 and 4.

Results

From Tables 2 and 4 where the data corresponds to a range of 2000' it is clear that for the first four cases the Honeywell LCOS, the AFAL LCOS, and AFALCOS are excellent while the advanced fighter sight is still very useable since the 3.4 mil error is well within the M-61 gun bullet dispersion pattern. When a high roll rate (p = .2 rad/sec) is introduced, however, the Honeywell LCOS, AFAL LCOS and advanced fighter sight introduce large errors--17.7 mils, 12.0 mils, and 21.5 mils respectively--because of the incorrect mechanization of the roll coupling in these sights. The AFALCOS for this case has an error of only 2.2 mils--an improvement by a factor of ten.

When the range is extended to 3000' for the first four cases, the LCOS sights degrade to an average radial error of 6.2 mils for Honeywell LCOS, 9.2 mils for AFAL LCOS, 10.2 mils for the advanced fighter LCOS, and 5.2 mils for AFALCOS.

When a roll rate of 0.2 rad/sec is introduced, the Honeywell LCOS, AFAL LCOS, and advanced fighter LCOS have an average radial error of 56.0 mils, 38.4 mils, and 66.8 mils respectively, while AFALCOS has a radial error of only 5.7 mils--again, an improvement by a factor of ten.

VI. CONCLUSIONS

(1) This report presents the derivation of the equations necessary to implement a lead computing optical sight in a fighter type aircraft. A fortran digital program is developed to implement these equations on a digital computer.

(2) The equations developed require the angular rate vector of the aircraft including the roll rate. These signals may be obtained from either a three axis strapdown gyroscope system or an inertial navigation system employing a stable platform. Use of either of these angular rate measuring devices will permit the elimination of the two axis lead computing gyroscope presently employed in LCOS.

(3) The assumptions leading to incorrect roll coupling in the Honeywell and the advanced fighter LCOS sights have been eliminated, and the roll coupling in AFALCOS now corresponds very closely in the steady state with the results of the HOTLINE historical tracer sight.

(4) In the comparisons made, in Tables 2, 3 and 4 the AFALCOS steady state radial error is less in almost every case than that of the Honeywell, advanced fighter and Avionics Lab LCOS sights. Therefore, when the HOTLINE sight is used as a steady state accuracy standard, AFALCOS is judged to be a more accurate sight than any other LCOS known to the authors.

(5) The digital code is not extensive for AFALCOS; hence, no particular programming difficulties are anticipated for airborne application.

(6) A word of caution--the numerical comparisons made in section V are steady state comparisons. Before final suitability of any lead computing sight can be established, the entire system including pilot, target, sight display, flight control system, and aerodynamic response of the aircraft, must be tested in a dynamic environment.

APPENDIX A

This appendix contains a listing of the Fortran digital code for AFALCOS. The input/output is structured to operate on a remote terminal of the Burroughs B6700 digital computer at the U. S. Air Force Academy.

```
C----  LEATHAM,A.L. USER CODE BYZ0185.  DFACS.  EXT. 2136
$RESET FREE
FILE  5=INPUT2,UNIT=DISK,BLOCKING=30,RECORD=14
FILE  7=LINE,UNIT=PRINTER
FILE  6=OUTPUT,UNIT=REMOTE,RECORD=22
 1000 FORMAT(1H0,F4.2,3F10.3,2F10.2)
 1001 FORMAT(1H0,'TIME',6X,'ELA',7X,'ALA',5X,'FLITIME',
     @2X,'ELHUD(MILS)',1X,'AZHUD(MILS)',//)
      REAL KB,JV
       NAMELIST/INPUT/P,Q,R,D,DDOT,VA,AX,AY,AZ,AL,GA,GAIN,DT,FTIME,HA
      @ ,VM,IPRINT
C
C  INPUT DATA
C
C  P,Q,R --- BODY ANGULAR RATES IN RADIANS/SEC
C  D,DDOT--- RANGE AND RANGE RATE IN FT AND FT/SEC
C  VA    --- AIRCRAFT SPEED IN FT/SEC
C  AX,AY,AZ- BODY ACCELEROMETER MEASURED ACCELERATION IN FT/SEC**2
C  AL,GA --- AIRCRAFT ANGLE OF ATTACK AND GUN ANGLE IN RADIANS
C  GAIN  --- SIGHT SENSITIVITY PARAMETER  .8 NOMINALLY
C  DT,FTIME- INTEGRATION STEP SIZE AND FINAL TIME IN SEC.
C  HA,VM --- ALTITUDE IN FEET AND MUZZLE SPEED IN FT/SEC.
C  IPRINT--- PRINT CONTROL INDEX
C
 500   READ(5,INPUT)
       PRINT INPUT
C  MCD ATMOSPHERE
       IF(HA.GT.36000.) GO TO 50
       RHO=(.034475+(.019213E-10*HA-.050381E-5)*HA)**2*2.
       S=1117.1-.00412778*HA
       GO TO 55
 50    DH=HA-36000.
       RHO=(.018828+(.039227E-10*DH-.043877E-5)*DH)**2*2.
       S=968.5
 55    DRATIO=RHO/.00238
       VP=VM+VA
       KB=.00614
       VLS=D*KB*VP**.5*DRATIO
       VC=-DDOT
       VOS=VM+VC-VLS
       VCM=(VOS**2-4.*(VA-VC)*VLS)**.5
       RTF=.5*(VOS+VCM)/D
```

```
C  TF IS BULLET TIME OF FLIGHT
      TF=1./RTF
      VF=D/TF-VC
      JV=(VM-VF)/(VA+VM)
C  B IS THE GUNLINE UNIT VECTOR IN BODY COORDINATES
      B1=COS(GA)
      B2=0.
      B3=SIN(GA)
C   AL IS THE A/C ANGLE OF ATTACK IN RADIANS, POS. FOR POS. LOAD FACTOR
C   GA IS THE GUN ANGLE MEASURED IN RADIANS DOWN FROM X AXIS
C  GAL IS THE GUN ANGLE OF ATTACK
      GAL=AL-GA
      C6=D+DDOT*TF
      C7=TF*D*P/2./C6
      C1=VF/C6
      C2=JV*VA/C6
      C3=TF/2./C6
      BXAN2=-B1*AZ+AX*B3
      BXAN3=B1*AY-AX*B2
      PRINT 1001
      PRINT 1000,T,ELA,ALA,TF,ELAH,ALAH
C  SL IS THE SIGHT LINE UNIT VECTOR
  100 SL1=B1+B2*ALA-B3*ELA
      SL2=B2-B1*ALA
      SL3=B3+B1*ELA
      W2=-C1*ELA-C2*GAL+C3*(BXAN2-(AY*ELA+AZ*ALA)*B2+(AX*B1+AY*B2+AZ*B3)
     @   *ELA)
      W3=-C1*ALA+C3*(BXAN3-(AY*ELA+AZ*ALA)*B3+(AX*B1+AY*B2+AZ*B3)*ALA)
      W2=W2+(-SL1*SL2+C7*SL3)*P+(1.-SL2**2)*Q-(SL2*SL3+C7*SL1)*R
      W3=W3-(SL1*SL3+C7*SL2)*P+(-SL2*SL3+C7*SL1)*Q+(1.-SL3**2)*R
       C5=C7*SL1
      DET=1.-SL2**2-SL3**2+C5**2
      AINVW2=((1.-SL3**2)*W2+(SL2*SL3+C5)*W3)/DET
      AINVW3=((SL2*SL3-C5)*W2+(1.-SL2**2)*W3)/DET
      DELA=GAIN*AINVW2
      DALA=GAIN*AINVW3
C  ELA AND ALA ARE EL. AND AZ. LEAD ANGLE COMPONENTS W.R.T. GUN
      ELA=ELA+DT*DELA
      ALA=ALA+DT*DALA
      T=T+DT
      ITIME=ITIME+1
      IF(ITIME.EQ.IPRINT) PRINT 1000,T,ELA,ALA,TF,ELAH,ALAH
      IF(ITIME.EQ.IPRINT) ITIME=0
C   ELAB AND ALAB ARE EL AND AZ LEAD ANGLES IN BODY COORDINATES
      ELAB=B1*ELA
      ALAB=B1*ALA
C  ELAH AND AZAH ARE HUD EL AND AZ ANGLES IN MILS.  HUD ANGLE=0.
      ELAH=-(ELA-HUDZ/(VF*TF)+GA)*1000.
      ALAH=-(ALA-HUDY/(VF*TF))*1000.
      IF(T.LT.FTIME) GO TO 100
      ELA=0.
      ALA=0.
      T=0.
      GO TO 500
      END
```

APPENDIX B

This appendix contains a listing of the Fortran digital code which represents the lead computing optical sight in an advanced fighter aircraft. The listing is a subroutine designed to operate in a larger program on the Burroughs B6700 computer at the U.S. Air Force Academy.

```
      SUBROUTINE F15LCO
      COMMON/HLLCOS/XHL,YHL,RHL,TOFHL
      COMMON/GUNDAT/H(150),S(300),TT(44),T
      COMMON/ANGLE/BPSI,BTHE,LEH,LAH,DELXX,DELYY,ELAH,ALAH,GAIN
      COMMON/SGYRO/AG,EG,SEG,CEG,SAG,CAG,DT
      COMMON/ICS/DX,DY,DZ,BKDRHO,BO,TAU,R1500,DELTA       ,PCY,PCZ,
     .ALCDFI,THE,PSI,  ALCDF,DELT,THG,ALOOP,RHO,VM,ATF
      REAL LAM,LAG,LEG,LAC,LEC,LAH,LEH
      EQUIVALENCE
     .(HA,S(24)),(VTAS,S(31)),(R  ,S(8)),
     .(VC,S(9)),(SAL,S(35)),(SBE ,S(36)),
     .(AXB,S(5)),(AYB,S(6)),(SA  ,S(7)),
     . (PP,S(2)),(QQ,S(3)),(RR,S(4)),
     .(ALPHA,S(201)),(BE,S(202))
      NAMELIST/DATTA/VTAS,R,HA,ALPHA,SA,SJ,PP,QQ,RR
     .,XRI,YRI,ZRI,XDOTP,YDOTP,HDOTP,XDOTE,YDOTE,HDOTE
      NAMELIST/OUTPUT/RHO,VLS,VOS,VCM,RTF,XI,VR,VCK,P,LAM,FG,
     .LEG,LAG,XH,YH,ZH,        CEG,CAG,SEG,SAG
C EMPERIALLY DERIVED BALLISTICS COEFF(FT/SEC)1/2
      IF(T.GT.0.06) GO TO 891
C IMTRALIZE SINES & COSINES OF AG & EG
      CAG=1.
      SAG=0.
      SEG=0.
      CEG=1.
      AG=0.
      EG=0.
  891 CONTINUE
      SSA=-SA
      ALPHH=ALPHA
      RHD=RHO/.00238
      BK=0.00614
C VELOCITY OF MISSILE(FT/SEC-1)
      VM=3300
      TAU=.25
CGUN ANGLE
      GA=0.0
      TGHE=0.0
```

```
C     TGHH IS THE SUM OF GUN ANGLE AND HUD ANGLE.
      TGHH=TGHE+GA
      SK=.714286
      DL=0.0
      DA=0.0
      DE=0.0
      TGHA=0.0
C COMPUTER CYCLE TIME IS DT
      DT=.06
 223  CONTINUE
      IF(VTAS .GT. 2000  .OR. VTAS .LE. 0)     VTAS=970
C COMPUTE INITIAL VELOCITY IN AIR MASS
    1 VP=VM+VTAS
C     AVERAGE VELOCITY LOST FOR STATIONARY TARGET.
      VLS=R*BK*SQRT(VP)*RHD
C     AVERAGE OVERTAKING VELOCTIY FOR STATIONARY TARGETS.
      VC=0.
      VOS=VM+VC-VLS
C VELOCITY CORRECTION FOR MOVING TARGET
      VCM=SQRT(VOS**2-4*(VTAS-VC)*VLS)
C RECIPROCAL OF TIME OF FLIGHT CALCULATION
      RTF=0.5*(VOS+VCM)/R
C     RECRIPROCAL OF SIGHT SENSITIVITY.
      RTN=RTF+TAU*VC*(RTF+VLS/R)/VCM
C DOME MAG CURRENT
      XI=RTN*SK
C     PROJECTILE AVERAGE RELATIVE VELOCITY.
      VR=RTF*R-VC
C     BALLISTIC CURVATURE COEFFICIENT.
      VCK=VTAS*(1-VM/VR)/VP
C     TOTAL GUN ANGLE OF ATTACK.
      ALPHAG=GA+ALPHH
C     PRECESSION RATE COMMAND.
      P=.5*(SSA+R*SJ/VTAS)/VR+RTN*VCK*ALPHAG
 222  CONTINUE
 100  CALL GSM(XI,P)
C     TOTAL LEAD ANGLE.
      LAM=ARCOS(CEG*CAG)*SK
      IF(ABS(SAG) .LE.1E-4)     GO TO 110
C     LEAD ANGLE ROTATION.
      FG=ATAN2(SEG/CEG,SAG)
      GO TO 120
  110 FG=3.1415926/2
C     GYRO AZIMUTH LEAD ANGLE.
 120  LAG=ATAN(COS(FG)*TAN(LAM))
      IF (ABS(LAG).LE.1.E-4) GO TO 130
C     GYRO ELEVATION LEAD ANGLE,
      LEG=ATAN(TAN(FG)*SIN(LAG))
      GO TO 140
 130  LEG=LAM
      IF (EG.LT.0.) LEG=-LAM
C     CORRECTED ELEVATION LEAD ANGLE.
 140  LEC=ATAN((1+DL/R)*TAN(LEG) -DE/R)
```

```
C     CORRECTED AZIMUTH LEAD ANGLE.
      LAC=ATAN((1+DL/R)*TAN(LAG)      +DA/R) +TGHA
C     HUD COORDINATES OF LEAD ANGLE
      XH=COS(LEC)*COS(LAC)*COS(TGHE)+SIN(LEC)*SIN(TGHE)
      YH=COS(LEC)*SIN(LAC)
      ZH=-COS(LEC)*COS(LAC)*SIN(TGHH)+SIN(LEC)*COS(TGHH)
C     HUD AZIMUTH LEAD ANGLE COMPONENT.
      LAH    =1000.*ATAN (YH/XH)
C     HUD ELEVATION LEAD ANGLE COMPONENT.
      LEH    =1000.*ATAN (ZH/XH)
  998 CONTINUE
  999 CONTINUE
      DELXX=LAH-BPSI
      DELYY=LEH-BTHE
 303  CONTINUE
      RETURN
      END
C LCG GYRO SIMULATION MODEL
C
CINPUTS
C XI - MAG CURRENT COMMAND
C XP - PRECESSION RATE COMMAND
C P  - ACFT ROLL RATE
C Q  - ACFT PITCH RATE
C R  - ACFT YAW RATE
C OUTPUTS
C AG - GYRO AZIMUTH GIMBAL ANGLE
C EG   GYRO ELEVATION GIMBAL ANGLE
C DEFINITIONS
C SG -GYRO SPACE ANGLE
C TG -GYRO TIME CONSTANT(SENSIVITY)
C TM - MODIFIED BYRO TIME CONSTANT
C TGL- GUNLINE ELEVATION ANGLE
C XG - GYRO ROLL RATE
C YG - GYRO PITCH RATE
C ZG - GYRO YAW RATE
C DT - COMPUTER CYCLE TIME
      SUBROUTINE GSM(XI,SP)
      COMMON/GUNDAT/H(150),S(300),TT(44),T
      COMMON/ANGLE/BPSI,BTHE,LEH,LAH,DELXX,DELYY,ALAH,ELAH,GAIN
      COMMON/SGYRO/AG,EG,SEG,CEG,SAG,CAG,DT
      COMMON/ICS/DX,DY,DZ,BKDRHO,BO,TAU,R1500,DELTA      ,PCY,PCZ,
     .ALCDFI,THE,PSI,  ALCDF,DELT,THG,ALOOP,RHO,VM,ATF
      REAL LAM,LAG,LEG,LAC,LEC,LAH,LEH
      EQUIVALENCE
     .(HA,S(24)),(VTAS,S(31)),(R  ,S(8)),
     .(VC,S(9)),(SAL,S(35)),(SBE ,S(36)),
     .(AXB,S(5)),(AYB,S(6)),(SA  ,S(7)),
     . (PP,S(2)),(QQ,S(3)),(RR,S(4)),
     .(ALPHA,S(201)),(BE,S(202))
 C P,Q,R IN.RAD/SEC
      NAMELIST/OUTT/XG,YG,ZG,SG,TG,SM,EGD,AGD,EG,AG,SAG,CAG,SEG,CEG
      TGL=0.
      XG=PP*COS(TGL)-RR*SIN(TGL)
```

```
      YG=QQ
      ZG=PP*SIN(TGL)+RR*COS(TGL)
      SG=ARCOS(CAG*CEG)
      IF (ABS(SG).LT.1.E-4) GO TO 80
      TG=(SG/1.4)/(XI*SIN(SG/1.4))
      SM=SG/SIN(SG)
90    EGD=XG*SIN(AG)-YG*COS(AG)-(COS(AG)*SIN(EG)/1.0)*(SM/TG)-SP
      AGD=-ZG-TAN(EG)*(XG*COS(AG)+YG*SIN(AG))-
     . (SIN(AG)/(COS(EG)*SIN(SG)))*(SG/TG)
      GO TO 100
80    EGD=XG*SIN(AG)-YG*COS(AG)-SP
      AGD=-ZG-TAN(EG)*(XG*COS(AG)+YG*SIN(AG))
100   EG=EG+EGD*DT
      AG=AG+AGD*DT
      SEG=SEG+EGD*DT*CEG
      CEG=CEG-EGD*DT*SEG
      SAG=SAG+AGD*DT*CAG
      CAG=CAG-AGD*DT*SAG
      RETURN
      END
```

APPENDIX C

This appendix contains a listing of the Fortran digital code for the Honeywell digital LCOS. The listing is a subroutine designed to operate in a larger program on the Burroughs B6700 computer at the U.S. Air Force Academy.

```
      SUBROUTINE LCOSS
      COMMON/HLLCOS/XHL,YHL,RHL,TOFHL
      COMMON/GUNDAT/H(150),S(300),TT(44),T
      COMMON/ANGLE/BPSI,BTHE,LEH,LAH,DELXX,DELYY,ELAH,ALAH,GAIN
      COMMON/SGYRO/AG,EG,SEG,CEG,SAG,CAG,DT
      COMMON/ICS/DX,DY,DZ,BKDRHO,BO,TAU,R1500,DELTA       ,PCY,PCZ,
     .ALCDFI,THE,PSI,  ALCDF,DELT,THG,ALOOP,RHO,VM,ATF
      REAL LAM,LAG,LEG,LAC,LEC,LAH,LEH
      EQUIVALENCE
     .(HA,S(24)),(V   ,S(31)),(RPA,S(8)),
     .(VC,S(9)),(SAL,S(35)),(SBE ,S(36)),
     .(AXB,S(5)),(AYB,S(6)),(ACGZ,S(7)),
     . (P ,S(2)),(Q ,S(3)),(R ,S(4)),
     .(AL,S(201)),(BE,S(202))
      IF (T.GT..06) GO TO 500
C     THG IS THE GUN ANGLE OF ATTACK
      THG=0.
C     DX,DY,DZ ARE DISTANCES FROM GUN TO HUD
      DX=0.
      DY=0.
      DZ=0.
C      BK IS AN EMPERICALLY DERIVED  ALLISTIC COEFFICIENT.
C      BKDRHO = BK/RHO = .00614/.00238.
       BKDRHO=2.58
       BO=.003713
C      TAU IS THE  AMPING FACTOR.
       TAU=.4
       TAU=.25
       R1500  = 1500.
C      R1500 IS THE FIXED RANGE WITH NO RADAR LOCK.
C      DELTA IS THE COMPUTER CYCLE TIME.
       PCY=0.0
       PCZ=0.0
       THE    = 0.
       PSI = 0.
       BPSI=0.
 211   BTHE=0.
       ALOOP=50.
       DELT=3.
  200 DELTA=DELT/ALOOP
```

```
C     VM IS THE MUZZLE VELOCITY
      VM=3300.
C     ALCDF=(1+TAU)*1.4
      ALCDF=1.25
C       ALCOFI = ( 1/(1+TAU) )
      ALCOFI=1./ALCDF
  500 CONTINUE
C     A393=0 INDICATES RADAR LOCK
      A393=0.
C     VTAS IS THE TRUE AIR SPEED.
      VTAS=V
      RANGE=R1500
      IF(A393  .EQ.0.) RANGE=RPA
      IF(RPA.LT.1.) RANGE=1.
  510 CONTINUE
C     THIS IS A VALIDITY CHECK.  RHO VS RANGE FOR CHECK.
      B=B0+(.000000888*(1255.-(V-VC)))
      SAVE=-.000000618*RANGE+B
      IF(RHO.LE.SAVE) GO TO 556
      RTN=.33333
      GO TO 557
  556 CONTINUE
      VP=VM+VTAS
C     VP IS INITAL PROJECTILE VELOCITY IN AIRMASS
      VLS=RANGE*BKDRHO*SQRT(VP)*RHO
      VC=0.
      VOS=VM+VC-VLS
      CHECK=VOS**2-4.*(VTAS-VC)*VLS
      VCM=SQRT(CHECK)
      VF=.5*(VOS+VCM)
C     VF IS AVERAGE PROJECTILE VELOCITY.
      RTF=VF/RANGE
C     RTF IS RECRIPROCAL OF TIME OF FLIGHT.
        ATF=1./RTF
      VR=RTF*RANGE-VC
      TFDOT=VC*(RTF+VLS/RANGE)/VCM
C     TFDOT  IS THE RATE OF CHANGE OF TOF/TF.
      RTN=RTF+TAU*TFDOT
C     RTN IS THE RECRIPROCAL OF SIGHT SENSITIVITY.
  557 TRTN=1./RTN
C     TRTN IS THE SIGHT SENSITIVITY.
      TF     = TRTN
      VT      = VM + V
C     VT IS THE TOTAL INITIAL PROJECTILE VELOCITY IN AIRMASS.
      VVT     =V/VT
      ALCPSI=ALCDF*PSI
      QXY=Q-P*ALCPSI
      RZG=R+ALCDF*THE*(P+Q*ALCPSI)
      RI=(VM-VR)/VR
      ALG    =RI*VVT
      ALG1    = (AL+THG)*ALG
      TF12=.5*TF
```

```
      PCY=RZG*TF
      ACCZ= ACGZ
      PCZ=QXY*TF    -ACCZ*TFI2/VR-ALG1
      XCAL=ALCDFI*DELTA/TF
      THE=THE-(THE+PCZ)*XCAL
      PSI=PSI-(PSI+PCY)*XCAL
      BPSI     = PSI      + DY/RANGE
      BTHE     = THE      - DZ/RANGE
     *-THG
      BPSI=1000.*BPSI
      BTHE=1000.*BTHE
      RETURN
      END
```

APPENDIX D

This appendix contains a listing of the Fortran digital code for the Air Force Avionics Laboratory digital LCOS. The code was extracted from reference [2]. The program is designed to be run from a remote terminal of the Burroughs B6700 computer at the U.S. Air Force Academy.

```
$RESET FREE
FILE  5=AVDATA,UNIT=DISK,BLOCKING=30,RECORD=14
FILE  6=OUTPUT,UNIT=REMOTE,RECORD=22
      REAL KBRHO,KH,KSIG,LE,LA,LAD,LED
       DIMENSION TME(205),PLE(205),PLA(205),IBUFF(1024)
 1    IPT=0
C THE FOLLOWING DATA REPRESENT INPUT VARIABLES
C CONSTANT INPUTS ARE ASSUMED HERE AS AN EXAMPLE
      NAMELIST/DATA/RANGE,VC,P,Q,R,AN,ALPHA,VA,RHO,HA
      READ(5,DATA)
      PRINT DATA
C RANGE IS IN FT
C VC IS NEGATIVE OF RANGE RATE IN FT/SEC
C P,Q,R ARE ANGULAR RATES OF AIRCRAFT IN BODY AXES, RAD/SEC
C AN IS NORMAL ACCELERATION IN FT/SEC/SEC (-32.17 WHEN STRAIGHT & LEVEL)
C ALPHA IS ANGLE OF ATTACK IN RADIANS
C VA IS TRUE AIRSPEED IN FT/SEC
C RHO IS AIR DENSITY IN SLUGS PER CUBIC FOOT
      TIME=0.
C SET CONSTANTS
C COMPUTER CYCLE TIME IS DT
      DT=.06
C SIG IS THE SIGHT DAMPING FACTOR
      SIG=0.4
      KSIG=1./(1.+SIG)
C VM IS MUZZLE VELOCITY IN FT/SEC
      VM=3300.
C KBRHO IS A BALLISTIC COEFFICIENT DIVIDED BY SEA LEVEL AIR DENSITY
      KBRHO=0.00614/.00238
C GA IS GUN ANGLE WITH RESPECT TO X AXIS OF AIRCRAFT
      GA=0.0
      COSGA=1.0
      SINGA=0.0
C RRH IS RECIPROCAL OF GUN HARMONIZATION RANGE
      RRH=.0005
C DA AND DE ARE Y AND Z DISTANCES OF GUN FROM HUD IN FT
      DA=0.
      DE=0.
CINITIALIZE
```

```
C IPRINT IS A PRINT CONTROL INDEX SET TO PRINT EVERY 5TH TIME INTERVAL
      IPRINT=0
      LA=C.
      LE=0.
      RDC=0.
      SQRV=SQRT(VA+VM)
      VLS=KBRHO*RHO*RANGE*SQRV
      VOS=VM+VC-VLS
      VCM=SQRT(VOS*VOS-4.*(VA-VC )*VLS)
      PRINT 10
 10   FORMAT(1HO,6X,'TIME',6X,'LA',7X,'LE',7X,'LAD',7X,'LED',7X,'WK',
     @7X,'WJ'//)
C END INITIALIZATION --- BEGIN LOOP
      DO 3 I=1,200
      IPT=IPT+1
      SLA=LA*(1.-.16667*LA*LA)
      SLE=LE*(1.-.16667*LE*LE)
      CLE=1.-.5*LE*LE
      CLA=1.-.5*LA*LA
      RCOS=1./(CLA*CLE)
      RDE=(-VC-RDC*SLE)*RCOS
      RE=RANGE*RCOS
C APPROXIMATION USED FOR SQUARE ROOT
C IF Y=APPROX. SQUARE ROOT OF X, THEN SQRT(X)=.5*(Y+X/Y) IS VERY CLOSE
      SQRV=.5*(SQRV+(VA+VM)/SQRV)
      VLS=KBRHO*RHO*RE*SQRV
      VOS=VM-RDE-VLS
C APPROXIMATION USED FOR SQUARE ROOT
C  RDE=-VC MAKES TOF CALCULATION IDENTICAL TO OTHER LCOSS.
      RDE=-VC
      VCM=.5*(VCM+(VOS*VOS-4.*(VA+RDE)*VLS)/VCM)
      VE=.5*(VOS+VCM)
C RTF AND VF ARE 1/TIME OF FLIGHT AND AVG RELATIVE VELOCITY OF BULLET
      RTF=VE/RE
      VF=VE+RDE
      RRANGE=1./RANGE
      KH=1.-RANGE*RRH
      VN=VF-SIG*RDE VLS*(VF+VA)/(VCM*VF)
      PG=P*COSGA-R*SINGA
      RG=P*SINGA+R*COSGA
      RDC=VA*(ALPHA+GA)*(VM-VF)/(VA+VM)+.5*AN/RTF
C WJ AND WK ARE COMPUTED SIGHT LINE ANGULAR RATES
      WK=(KH*DA*CLA*RTF-VN*SLA)*RRANGE
      WJ=((RDC-KH*DE*RTF)*CLE-VN*CLA*SLE)*RRANGE
      LED=(WJ+SLA*PG-CLA*Q)*KSIG
      LAD=((WK-SLE*(CLA*PG+SLA*Q))/CLE-RG)*KSIG
      LA=LA+LAD*DT
      LE=LE+LED*DT
```

```
C LA AND LE ARE AZIMUTH AND ELEVATION ANGLES OF COMPUTED SIGHT LINE
C LA AND LE ARE IN RADIANS. COMPUTE PLA AND PLE AS NEGATIVE IN MILS
      PLA(IPT)=-1000.*LA
      PLE(IPT)=-1000.*LE
      TIME=TIME+DT
      TME(IPT)=TIME
      IPRINT=IPRINT+1
      IF(IPRINT.NE.25) GO TO 3
      PRINT 11,TIME,LA,LE,LAD,LED,WK,WJ
      IPRINT=0
   11 FORMAT(1X,F10.3,4F10.6,2F10.6)
    3 CONTINUE
      TOF=1./RTF
      NAMELIST/DEBUG/TOF,VF,VE,VCM,VOS,VLS
      PRINT DEBUG
      GO TO 1
      END
```

REFERENCES

1. F-4E Lead Computing Optical Sight System (LCOSS) Improvement Study, Report MDC A0610 1 June 1971, Mc Donnell Aircraft Company, St Louis, Missouri.

2. Air-to-Air Gun Fire Control Equations for Digital Lead Computing Optical Sights, by R.A. Manske, AFAL-TM-74-9-NVE-1, Apr 1974, Air Force Avionics Laboratory, Wright-Patterson AFB, Ohio.